

Project Description:

The main objective of this proposed research is to *provide state DOTs a practical and cost-effective long-term fatigue crack monitoring methodology using a **wireless elastomeric skin sensor network***. This research is intended to demonstrate the value-added of fatigue crack monitoring of steel bridges using wireless skin sensors over the traditional bridge inspection.

Progress this Quarter (includes meetings, work plan status, contract status, significant progress, etc.):*ISU Progress:*

Under this task, fatigue crack sensors are to be produced with an approximate thickness of 100-200 μm to enhance the mechanical robustness under harsh environment. Acceptable range of capacitance is 800-1000 pF. The anticipated number of sensors is 150 to 200 for the duration of the project.

During this quarter, the research efforts have been focused on ameliorating the mix to provide even more cost-effective alternatives. In particular, we have looked at adjusting the electrode mix in order to provide a uniform conductive layer that could be spray-painted. Technical support (Task 3) is being provided to KU on a continuous basis, as well as discussion and feedback (Task 4).

KU Progress:

KU evaluated the signal from the small SECs as well as SECs which are folded 90 degrees using the bridge girder subassembly model. Two sensor arrays were installed in the bridge model and preliminary test results were obtained. The data show promising results of crack detection under distortion-induced fatigue crack using a combination of SECs deployed over flat as well as 90-degree surfaces.

KU is also currently working with KDOT to identify a steel bridge to serve as the field testbed for the project.

UA Progress:

Arizona team has been focused on sensor board noise improvement under 3.2V supply and interface work with Xnode wireless sensor platform. In general the sensor board performances are equivalent with ones of a commercial wired capacitance measurement toolkit (PCAP). Unintended flipping signals have been observed as parts of the noises during the tests. It turns out that the flipping signals are not from the sensor board but real capacitance variation by comparison tests with the PCAP. Further investigations may be required, but it may be due to improper installation of the SEC sensor to the steel plate or buckling phenomenon of the SEC patch during the plate bending tests.

Xnode sensor module was tested with our sensor board. Xnode has eight channels designed for acceleration, strain, voltage and temperature measurements. Calibration and comparison test were conducted via 7th channel of the Xnode, which allow voltage measurement from 0V to 2.4. The calibration test results have shown good agreement with commercial wired data acquisition system (i.e NI DAQ).

Anticipated work next quarter:

ISU: Sensor production will continue in the next quarter. Technical support is being provided to KU on a continuous basis, as well as discussion and feedback.

KU: KU team will continue to test the bridge subassembly model and propagate the crack. The collected data will be analyzed and used to create algorithms to detect out-of-plan cracks using the SEC arrays.

UA: In the next quarter, Arizona team will continue on more extensive tests in combination with the Xnode and possible hardware improvement.

Significant Results:

Part 1: Crack detection using the SEC sensor

The KU team continued to focus on testing SECs on the bridge-girder-to-cross-frame subassembly in this quarter. In particular, two tasks have been conducted: 1) checking small SEC sensor's signal; and 2) finishing sensor network installation on the subassembly and getting preliminary testing results from the SECs.

1.1 Checking small SECs' signal

As shown in the report of last quarter, an SEC sensor array was proposed for monitoring fatigue crack of the bridge girder subassembly model. The sensor array was a combination of SECs with small and large sizes. The small SEC, with the dimensions of 1.5 in. × 1.5 in., was tested for the first time in this project. Before formally running the test model with small SECs, it is critical to check the small SEC's signal as well as the functionality of the data acquisition (DAQ) system.

Another objective of this test is to evaluate whether the SEC would produce reliable signal when folded 90 degrees between the girder web and stiffener, where fatigue cracks are found in the subassembly model. The ability for the SEC to work under folded condition is critical to the success of the test.

Fig.1 shows the test setup. To check the signal, small SECs were not installed at crack-critical locations. Instead, sensor 1 and 2 were installed on the top chord of the cross frame. Sensor 3 and 4 were installed at the diagonal brace of the cross frame. Sensor 5 and 6 were folded 90 degrees and installed between the girder web and the stiffener.

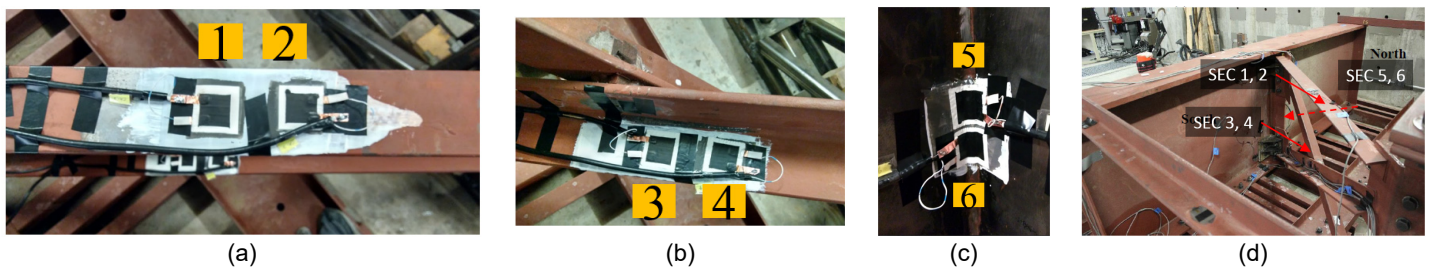
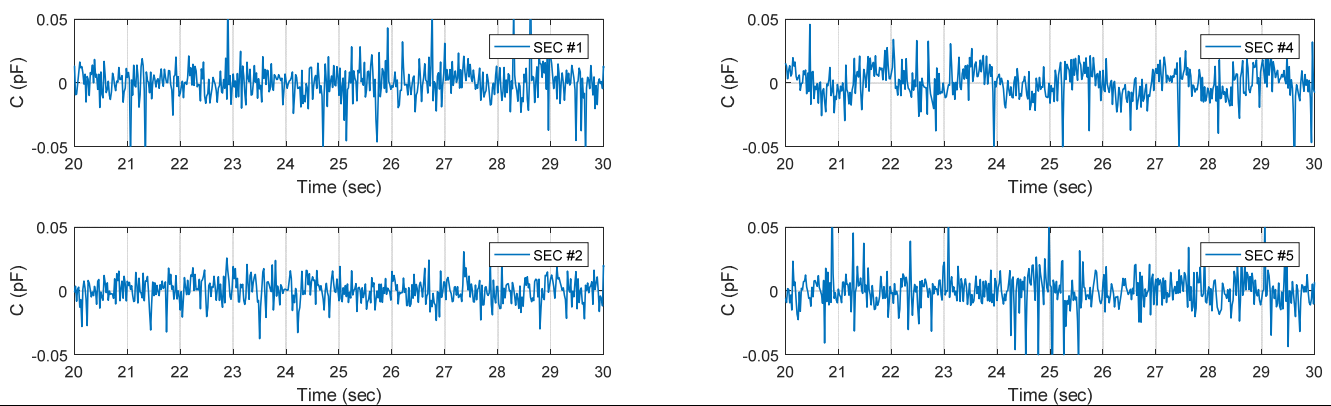


Fig. 1 Small SEC installation: (a) sensor 1, 2; (b) sensor 3, 4; (c) sensor 5, 6; and (d) locations of sensors in the subassembly model

Sinusoidal load cycles with a load range from 0 to 2.5 kip and a loading rate of 0.5 Hz were applied in the test. Short-time measurements of small SECs were collected under the loading cycles. Fig. 2 shows the signals of all 6 small SECs for a 10-sec duration. Despite noise content in the time-domain signal, a 0.5 Hz periodic signal can be observed from most small SECs.

Fig. 3 presents the power spectral densities (PSD) of all SEC measurements. A dominant peak occurred around 0.5 Hz which is the loading rate. The peaks in frequency domain verify the 0.5Hz sinusoidal signal measured from the small SECs.

Results shown in Fig. 2 and Fig. 3 indicate the small SECs' ability for monitoring strain change under cyclic loading. Furthermore, results from sensor 5 and 6 verify the SECs' functionality when folded 90 degrees.



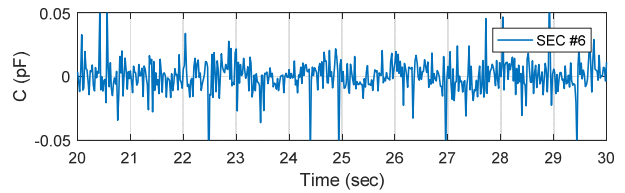
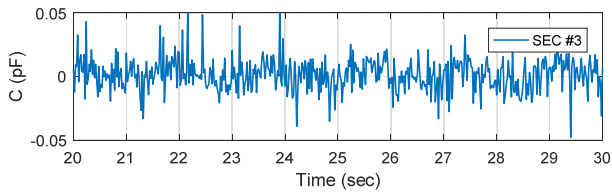


Fig. 2 Signals from small SECs: from sensor 1 to 6

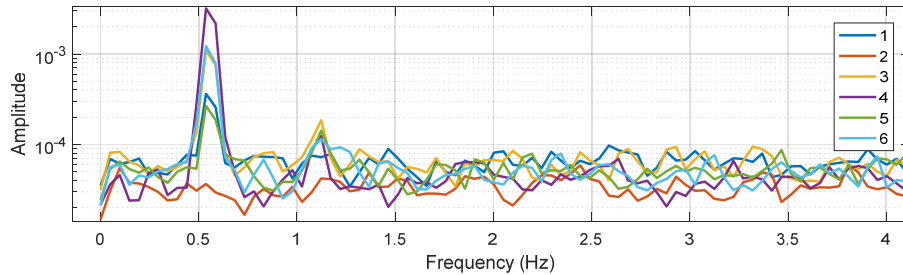


Fig. 3 PSD of all SECs

1.2. Preliminary testing results from the bridge subassembly model

Once the small SEC's signal has been verified, the KU team continued to complete the sensor installation and cabling on the test model, then ran the test, collected the measurements, and analyzed the test data.

Fig 4a shows the bridge subassembly model. SEC arrays were attached to cover the existing fatigue cracks and adjacent areas to monitoring the crack growth. Fig 4b and 4c show the SEC arrangement at the top of the connection. A total of 11 SECs with different sizes were installed: sensor a3, a7, a8 were at the stiffener side; sensor a2, a6, a9, and a11 were on the girder web side; and sensor a1, a5, and a10 were folded 90 degrees between the stiffener and the girder web. Similarly, Fig. 4d and Fig. 4e illustrate the SEC arrangement at the bottom of the connection. At the time of running this test model, existing out-of-plan fatigue cracks can be found at both ends of the connection. The crack tips are indicated by red crosses in Fig. 4c and Fig. 4e.

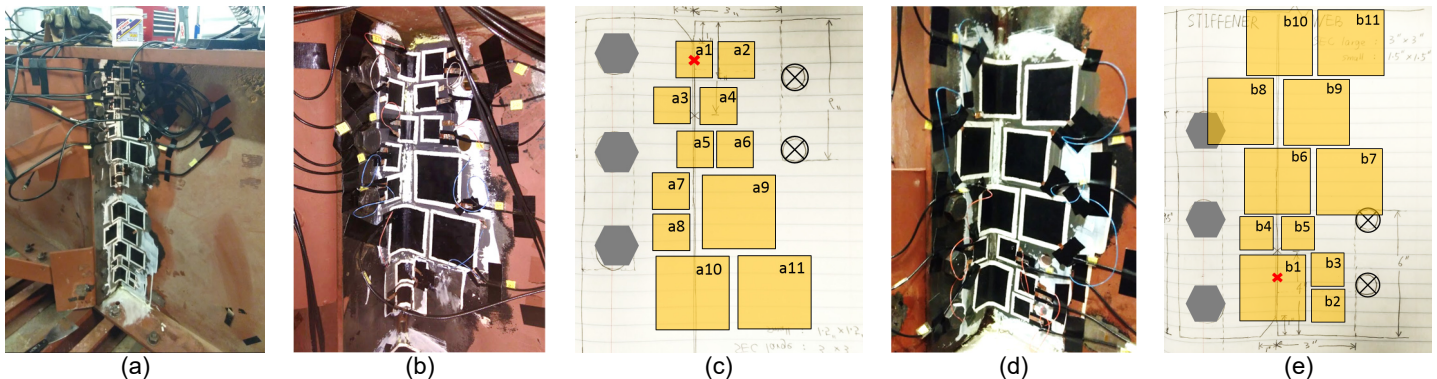


Fig. 4 (a) An overview of the bridge girder to cross frame connection; (b) top of the connect; (c) sensor arrangement map at top of the connection; and (d) bottom of the connection; and (e) sensor arrangement map at bottom of the connection

Previously, the KU team developed a crack monitoring algorithm of the SEC and validated the algorithm using compact, C(T), specimens. For the bridge girder to cross frame connection model, the same approach was applied to extract the crack growth index (CGI) from the SEC measurements.

In order to evaluate the CGI under different load ranges, different sinusoidal load cycles were applied. Table 1 shows the matrix of loading protocols applied in this test. A total of 5 sets of SEC measurements were collected. All load cycles were under a 0.5 Hz loading rate. Datasets 1 and 2 were collected under the same load range but at different times; dataset 3 to 5 were collected under lower load ranges. The applied loads were also recorded along with the SEC measurements.

Table 1 Loading protocol

Dataset	Load range
1	0 – 2.4 kip
2	0 – 2.4 kip
3	0 – 1.28 kip
4	0 – 2 kip
5	0 – 0.76 kip

Typical SECs' responses from dataset 1 are shown in Fig. 5, taken under 0 to 2.4 kip load range. The signals are grouped into four figures: 1) small SECs a1 to a7 at the top of the connection; 2) SEC a8 with other small SECs b2 to b5 at the bottom of the connection; 3) three large SECs a9 to a11 at the top of the connection; and 4) all large SEC b1, b6 to b11 at the bottom of the connection.

Generally speaking, most SECs produce cyclic responses under the applied load, varying the SEC array's ability to measure the structural response over a large surface. In particular, SEC a1 in Fig. 5a demonstrates larger response than other SECs. This is due to the large deformation under SEC a1 caused by cracking. Large SECs have higher noise content compared with small SECs.

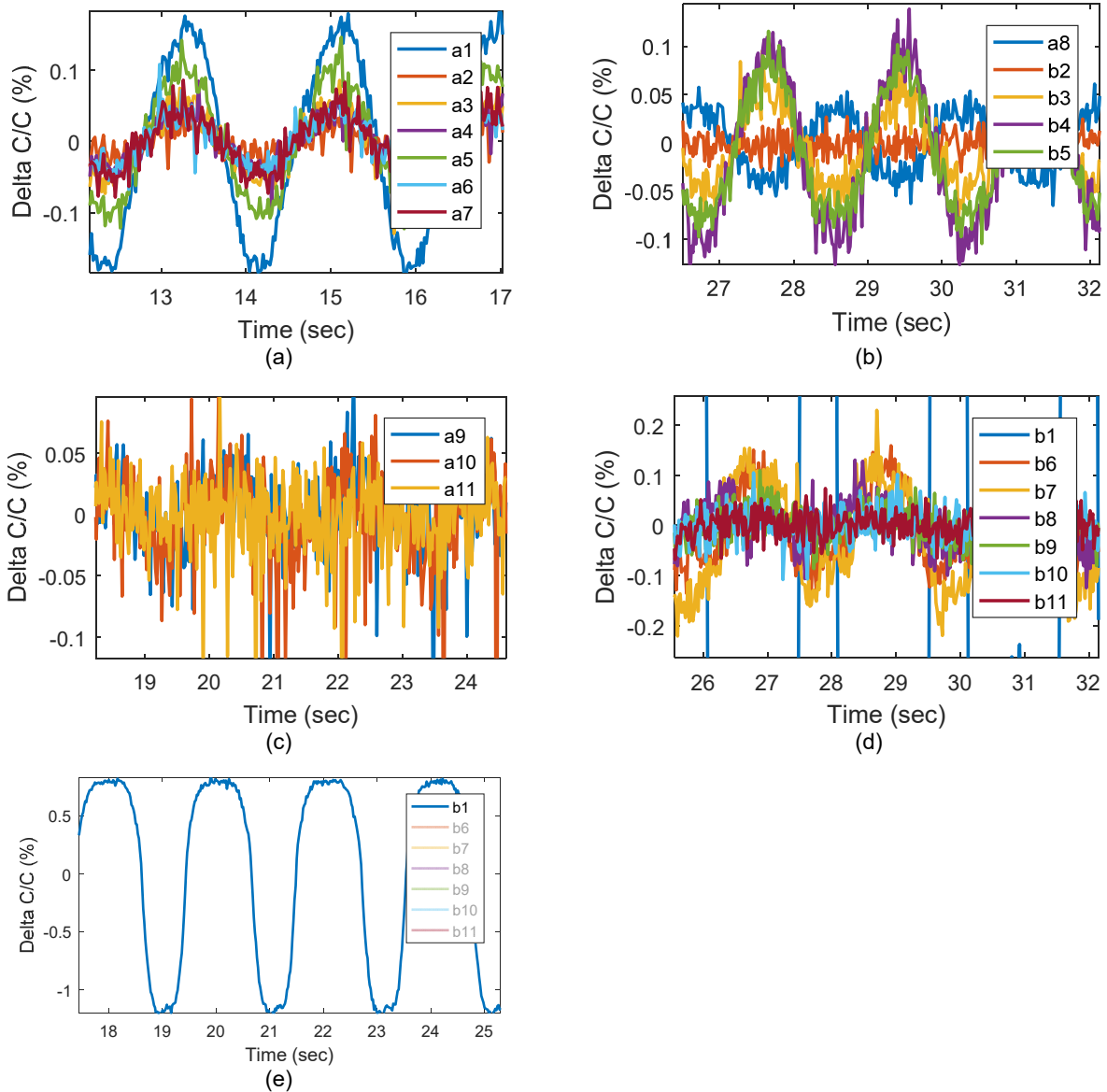


Fig. 5 CGI at the top of the connection

During the test, a crack was found in the top conductive layer of SEC b1 due to the significant deformation caused by the fatigue crack of the bridge model. As a result, a different signal pattern was found in Fig. 5e under a load range from 0 to 0.7 kip. The SEC b1 showed a very large capacitance response, which could potentially be used as a signature pattern for identifying fatigue crack.

After taking all five dataset in table 1, the crack monitoring algorithm was applied to compute the CGI. Fig. 6 shows CGIs of all SEC's measurement at the top of the connection under varying load ranges. Several observations can be obtained from the figure:

- SEC a1 has the largest response which leads to the highest CGI (about 0.5) than any other SECs. This indicates that the small SEC at the very top of the connection can capture the fatigue crack. CGIs on other SECs show a decreasing trend when the sensor was deployed lower (i.e. far away) from the tip of the fatigue crack.
- In Fig 5b, a2 has the lowest CGI response among all SECs. This behavior indicates the strain field covered by SEC a2 drops caused by fatigue crack growth.
- Shown in Fig. 5c, SEC a5 exhibits the larger CGI than SEC a6 to a8, this is due to the fact that SEC a5 is subject to the rotation effect between the stiffener and the web. Such a rotation behavior may provoke additional SEC response comparing with flat SECs in other locations.
- SEC a1 and a10 in Fig. 5d show nonlinearity in CGI under different load ranges, while other SECs mainly produce constant CGIs. This may be caused by the rotation between the stiffener and the web. In particular, the SEC's response may have nonlinear behavior under different magnitudes of rotation under the applied load.

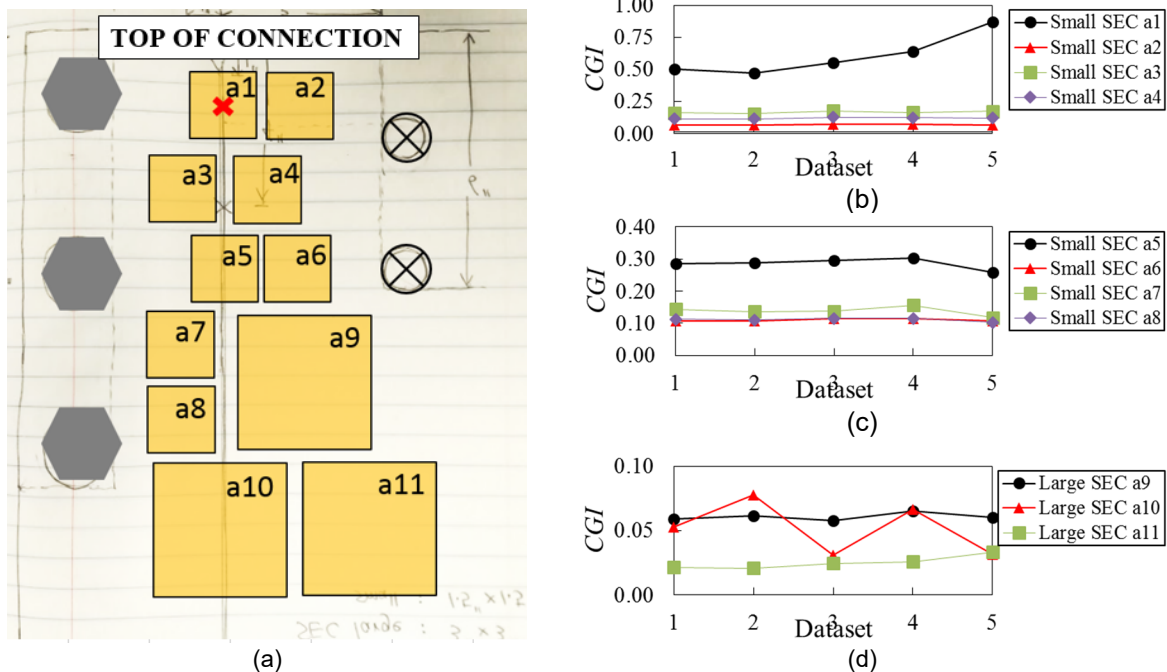
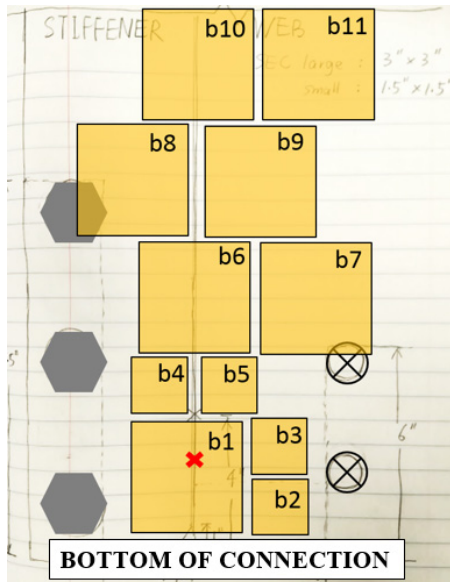
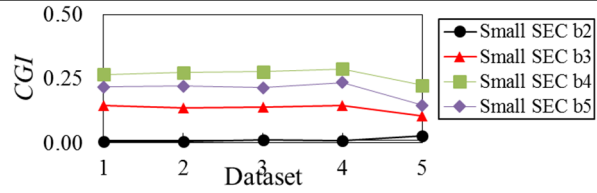


Fig. 6 CGIs from the SECs at the top of the connection

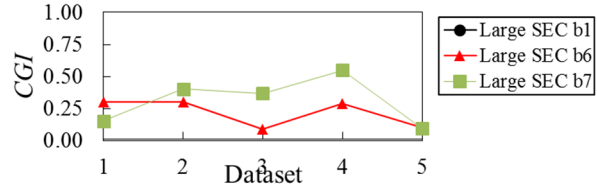
Fig. 6 shows the CGI results at the bottom of the connection. Similar trends can be observed from Fig. 6b to 6d. The CGI of SEC b1 was not shown in Fig. 6c. This is because the SEC b1 experienced a much larger deformation under a longer fatigue crack and a larger crack opening, leading to potential damage (i.e. cracking) to the sensing material. Under this situation, the SEC b1 produced a much larger CGI that is out of the range in Fig. 6c.



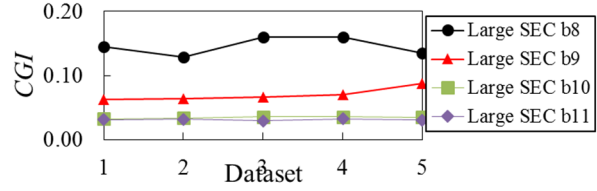
(a)



(b)



(c)



(d)

Fig. 6 CGI at the top of the connection

As a summary of the preliminary test results, the fatigue crack in the bridge subassembly model can be detected through CGIs from a large-area SEC array. SECs covering a fatigue crack produced higher CGIs, while CGIs of SECs at other locations showed the level of strain. Combination of these two types of sensors can potentially provide a comprehensive understanding of the structural response under fatigue cracks.

Part 2: Wireless data acquisition

The main results from the University of Arizona team are presented as follows.

Unintended signal flipping has been observed under sinusoidal load during tests as shown in Fig. 7.

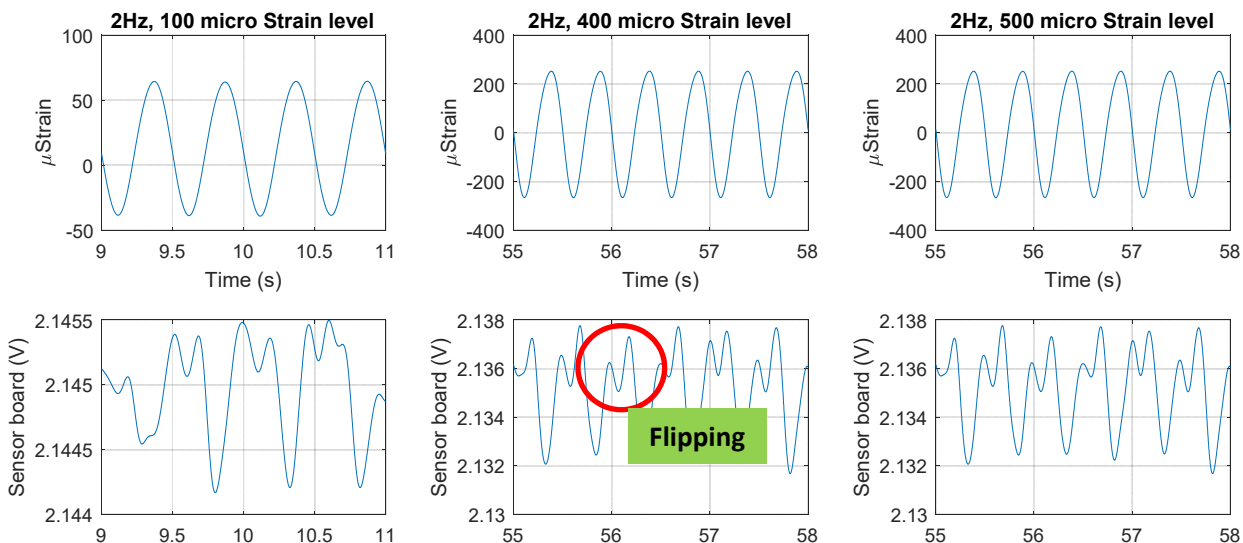


Fig. 7. Test result showing unintended flipping

A comparison test was conducted to figure out the source of the unintended flipping signals, whether from the sensor board or the specimen, by using the commercial DAQ (i.e. PCAP). Because one SEC sensor's capacitance cannot be measured by multiple DAQs, this test was done by quickly changing measuring devices (i.e. sensor board & PCAP) while keeping the

constant excitation. Fig. 8 shows the test setup. A cantilevered plate was constrained at the top to make an intended bending deformation using the shake table, minimizing the plate dynamics.

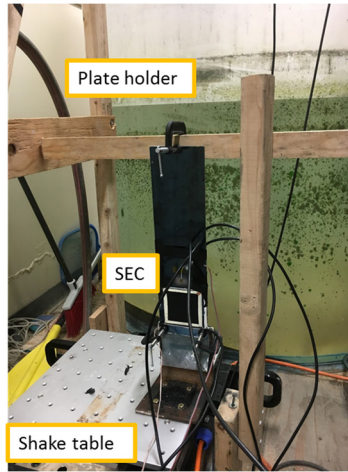


Fig. 8 Test setup

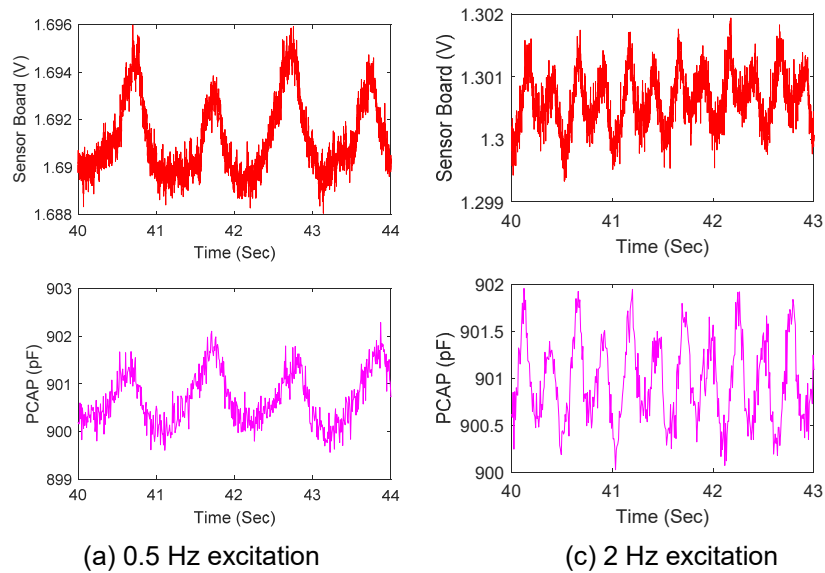
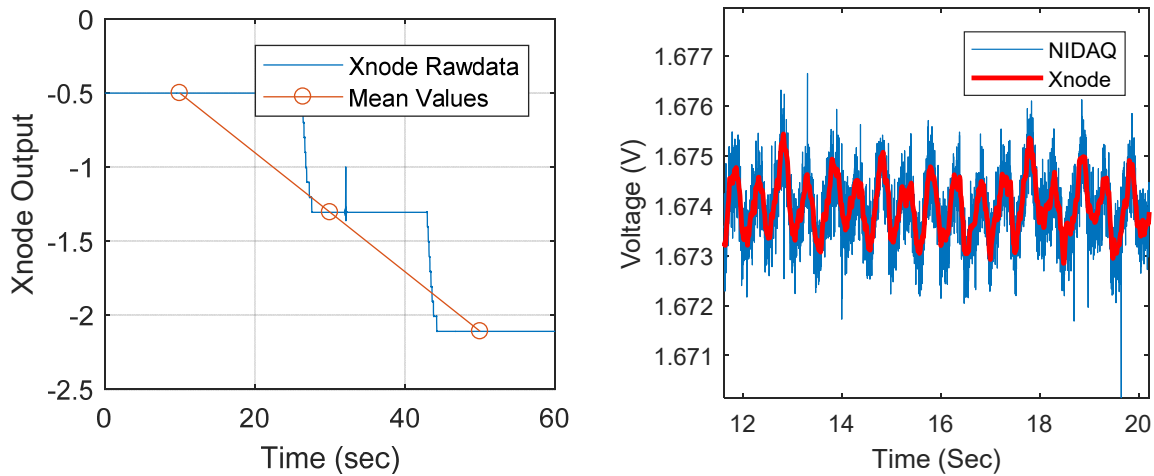


Fig. 9 Comparison test result: Sensor board measurement (top row) vs. PCAP measurement (bottom row)

Fig. 3 shows the comparison test results under 0.5Hz and 2Hz sine excitations. Results show similar signal shapes from both the sensor board and PCAP. Both signals include another unintended frequency components leading to twice of the original excitation frequency. Comparison test results confirmed that flipping is not from the sensor board but reflects actual capacitance variation. Further investigation may be required, but possible sources of such flipping signal may be due to bending buckling of the plate under the test setup.

Regarding the wireless sensor platform, the Xnode interface has been calibrated and tested with the sensor board. Xnode has total 8 channels: 3-Acceleration, 3-Strain, 1-voltage, and 1-temperature. Voltage measurement with 0-2.4V range is supported.



(a) Calibration test result; (b) Comparison with NIDAQ measurement
 Fig. 10 Xnode Calibration and comparison test result

Fig. 10(a) shows the calibration test done by changing the voltage supply as 0.5V-1.3V-2.1V for each 20 sec. The calculated calibration factor was -1 using averaged values of each steps and a linear relationship is observed. Fig. 10(b) shows the comparison test result between NIDAQ and Xnode. They show good agreement. The noise content from NIDAQ is due to the high sampling frequency. Sampling frequency of NIDAQ was 1kHz but, while Xnode was sampling at 100Hz.

Circumstance affecting project or budget. (Please describe any challenges encountered or anticipated that might affect the completion of the project within the time, scope and fiscal constraints set forth in the agreement, along with recommended solutions to those problems).

None.